



Available online at www.sciencedirect.com

ScienceDirect

Acta

Geochimica et

Cosmochimica

Geochimica et Cosmochimica Acta 333 (2022) 39-55

www.elsevier.com/locate/gca

Potassium isotope fractionation during chemical weathering in humid and arid Hawaiian regoliths

Wenshuai Li^{a,1}, Xiao-Ming Liu^{a,*}, Yan Hu^{b,2}, Fang-Zhen Teng^b, Oliver A. Chadwick^c

Department of Earth, Marine and Environmental Sciences, University of North Carolina, Chapel Hill, NC, USA
 Isotope Laboratory, Department of Earth and Space Sciences, University of Washington, Seattle, WA, USA
 Department of Geography, University of Calaifornia, Santa Barbara, CA, USA

Received 7 October 2021; accepted in revised form 1 July 2022; available online 8 July 2022

Abstract

The controls on potassium (K) isotope fractionation during chemical weathering are evaluated using two regolith profiles developed over ~350 kyr on the humid and arid sides of Kohala Mountain, Hawai'i. The humid regolith shows 145% K enrichment relative to the basaltic parent in shallow (≤1 m) horizons, but losses of up to 90% in the deeper horizons. By contrast, the arid regolith has lost between 60 and 90% K from the top 1 m of the soil with the least depletion in the deeper horizons due to limited chemical weathering. This apparent contradiction can be explained by enhanced accumulation of K-bearing mineral aerosols in the humid regolith. Bulk δ^{41} K varies from -0.76 ± 0.08 to $-0.31 \pm 0.06\%$ in the humid regolith compared with -0.48% for the underlying basalt. In contrast, the arid regolith shows $\delta^{41}K$ values ranging from -0.39 \pm 0.10 to $-0.02 \pm 0.05\%$, heavier than that of their basaltic parent. Exchangeable (NH₄Ac extracts) δ^{41} K of the humid and arid regoliths ranges from -0.63 ± 0.07 to $0.11\pm0.07\%$ and -0.01 ± 0.05 to $0.04\pm0.08\%$, respectively. Exchangeable K has δ^{41} K higher than (or similar to) the bulk values in most samples, reflecting a potential contribution of marine aerosols to the labile (plant available) K pool. In the shallow regolith, K derived from mineral aerosols is significant, especially for the humid site, and this idea is supported by enriched quartz, radiogenic Nd-Sr isotope values towards the surface, and increasing δ^{41} K close to the upper crustal composition (an analogue of the dust). The enrichment of K in humid surface soils, an upward decrease in exchangeable $\delta^{41}K$ in the humid regolith and plant-like $\delta^{41}K$ in the topmost, organic-rich soils may reveal the contribution of plant cycling. Low $\delta^{41}K$ in deep, humid regolith relative to $\delta^{41}K_{Basalt}$ appears to be driven by clay incorporation of isotopically light K. In comparison, higher δ^{41} K in the arid regolith than δ^{41} K_{Basalt} likely reflects an interplay between preferential clay 41K sorption in alkaline environments and preservation of seawater-derived K in forms of clay adsorbed complex and carbonate phases (via adsorption and/or incorporation). Our results reveal that the K isotope composition in Hawaiian regoliths depends on climate, while it is complicated by the interaction among weathering, plant cycling and addition of marine and mineral aerosols.

© 2022 Elsevier Ltd. All rights reserved.

Keywords: Basalt; Soil; Island; Ecosystem; Climate

Abbreviations: XRD, X-Ray diffraction; MAP, mean annual precipitation; UCC, upper continental crust; NH4Ac-K, regolith K extracted by NH_4Ac , also known as exchangeable K

^{*} Corresponding author.

E-mail address: xiaomliu@unc.edu (X.-M. Liu).

¹ Present address: Department of Earth and Planetary Science, Graduate School of Sciences, University of Tokyo, Tokyo, Japan.

² Present address: Université de Paris, Institut de Physique du Globe de Paris, CNRS, 1 rue Jussieu, Paris, France.

1. INTRODUCTION

Chemical weathering is one of the primary drivers for multiple geological processes, including (1) shaping planetary topography, (2) promoting soil formation, (3) regulating terrestrial nutrient supplies to the oceans, and (4) modulating atmospheric CO₂ and carbon cycles (e.g., Dupré et al., 2003; Royer et al., 2007). Chemical weathering could promote the cycling of elements between the atmosphere, hydrosphere, lithosphere, and biosphere (Lasaga et al., 1994; Riebe et al., 2001; Vance et al., 2009). Chemical weathering is the primary mechanism by which atmospheric CO₂ is removed over geological timescales. Constraining the intensity (i.e., the degree of weathering alteration and decomposition of rocks and minerals) and rate (the amount of change in weathered materials per unit time) of chemical weathering using robust proxies is necessary to trace climate change over geological timescales (Liu and Rudnick, 2011; Dupré et al., 2003; Royer et al., 2007; Vigier and Goddéris, 2015). Commonly used weathering tracers include Sr (⁸⁷Sr/⁸⁶Sr) and Os (¹⁸⁷Os/¹⁸⁸Os) isotopes. For example, the changes in seawater ⁸⁷Sr/⁸⁶Sr and ¹⁸⁷Os/¹⁸⁸Os values over the Cenozoic can be linked to increases in silicate weathering intensity/flux, in response to tectonic uplifts (e.g., DePaolo, 1986; Hodell et al., 1990; Ravizza, 1993; Peucker-Ehrenbrink et al., 1995). However, ⁸⁷Sr/⁸⁶Sr and ¹⁸⁷Os/¹⁸⁸Os of various lithologies can be highly variable at both spatial and temporal scales, thus complicating the interpretation of chemical weathering (Pierson-Wickmann et al., 2002; Bataille et al., 2017). Therefore, we require multiple proxies to better understand continental weathering.

Recent analytical advances enable accurate measurement of stable potassium isotope ratio (41K/39K) using MC-ICP-MS to detect K isotope fractionations with high analytical precision (up to 0.06%, 2 S.D.) (Wang and Jacobsen, 2016, Li et al., 2016; Hu et al., 2018; Morgan et al., 2018, Chen et al., 2019; X. Li et al., 2020; Moynier et al., 2021; An et al., 2022; Zheng et al., 2022a). Potassium isotopes are ideal for tracing silicate weathering because K is a major alkali element in crustal rocks and can be systematically mobilized during silicate weathering. In addition, magmatic differentiation causes no analytically resolvable isotopic fractionation and igneous rocks generally have a narrow δ⁴¹K range (Morgan et al., 2018; Tuller-Ross et al., 2019; Hu et al., 2021). By contrast, recent studies of plants, river waters, seawater, and sediments show that K isotopes are substantially fractionated (up to \sim 2‰) at Earth's surface. For example, clays preferentially incorporate ³⁹K into their structure, with ⁴¹K being partitioned to waters or on clay surfaces, and isotopic fractionation driven by clay formation processes may reach to >1% (e.g., S. Li et al., 2019; Li et al., 2021a, 2021b; X. Li et al., 2022). The δ^{41} K of the bulk silicate Earth (BSE, -0.48%) and upper continental crust (UCC, ave. -0.44%) are about 0.5% lower than that of modern seawater ($\sim 0.14\%$) (Wang and Jacobsen, 2016; Hille et al., 2019; Wang et al., 2020; Huang et al., 2020; Teng et al., 2020), primarily due to a combination of continental weathering and marine hydrothermal contribution (S. Li et al., 2019; Hu et al.,

2020; Zheng et al., 2022b). Potassium isotopes are strongly fractionated by biological activities with preferential ³⁹K uptake by biomass (Christensen et al., 2018; Li et al., 2021c; Li et al., 2022a; Li et al., 2022b). The fact that ~90% of K in global river dissolved loads is sourced from silicate weathering (Meybeck, 1987; Berner and Berner, 2012; Wang et al., 2021; X. Li et al., 2022) does not preclude the possibility that K is biologically cycled and isotopically fractionated before ending up in rivers. Therefore, the measurement of K isotopes on Earth's surface probably needs the consideration of biogeochemical effects.

Regolith provides complex terrestrial records of geological changes in response to chemical, physical, and biological processes occurring at Earth's surface. To better constrain the use of K isotopes, we need to clarify the mechanism(s) producing the variation in regolith δ^{41} K. Previous studies focused on the impact of chemical weathering on δ⁴¹K in deep saprolites (excluding soil layers where open chemical system behavior is the most complex) (Chen et al., 2019; Teng et al., 2020). Broadly, weathering of terrestrial rocks leaves an isotopically lighter regolith, balancing heavier K isotope composition in rivers. Nevertheless, K accumulation (or depletion) and δ^{41} K values in the regolith are determined by poorly constrained interactions among atmospheric inputs, chemical weathering, and biological cycling. Moreover, the key controls under different climate conditions may vary significantly. This study evaluates potential factors responsible for changes in K element chemistry and δ^{41} K during regolith development in contrasting climate conditions, including a humid (mean annual precipitation, MAP $\sim 1730 \text{ mm}\cdot\text{yr}^{-1}$) and an arid site (~380 mm·yr⁻¹) on the Island of Hawai'i (Hawai'i digital rainfall map; Giambelluca et al. 2013). We measured δ⁴¹K of bulk samples, basaltic substrate, NH₄Ac extracts, and rainwater, combined with radiogenic Nd and Sr isotope composition to provide a comprehensive interpretation of K isotope behaviors during chemical weathering.

2. GEOLOGICAL BACKGROUND

Kohala Mountain is the northwestern-most and oldest volcano making up Hawai'i Island (McDougall, 1964). It has a tropical, mountainous-oceanic climate, producing a strong windward-leeward rainfall contrast, which is useful for assessing climatic impacts on weathering alteration (Chadwick et al., 2003). There are two aerially exposed lavas showing different physicochemical features on Kohala Peninsula. The most geographically and volumetrically extensive one is the Pololū lava, principally composed of tholeiitic basalts (\sim 350 kyr in age), while the Hāwī lava forms an alkalic cap covering the entire central region (~150 kyr in age) (e.g., Spengler and Garcia, 1988; Chadwick et al., 2003). The products from the Hawi and Pololū volcanisms are isotopically similar in radiogenic Nd-Sr isotopes and have comparable elemental ratios (e.g., K/Nb and K/Rb) and δ^{41} K compositions (Tables 1 and S1). We sampled two regolith profiles on minimally eroded locations on the Pololū flows. The two sites receive distinct mean annual rainfall, which were characterized in Goodfellow et al. (2014). The ages of the regoliths forming on these lavas are difficult to constrain. We considered the radiometric ages of the lavas to be equivalent to the duration of chemical weathering (~350 kyr) because the constructional surface of the Pololū flows was minimally eroded only (e.g., Goodfellow et al., 2014; Li et al., 2020). Sporadic volcanic debris can be observed in soils, which may be ascribed to the deposition of volcanic tephra during the more recent Hāwī eruptions (~150 kyr, Moore and Clague, 1992). Because the Hāwī and Pololū volcanisms are chemically similar and Hāwī tephra may have been incorporated into the older Pololū soils, they are not distinguished in this study and collectively called "the basaltic substrate" of the studied Hawaiian regoliths (Li et al., 2020).

The humid (BE, MAP of $1730 \pm 57 \text{ mm} \cdot \text{yr}^{-1}$) and arid (PO, MAP of $385 \pm 53 \text{ mm} \cdot \text{yr}^{-1}$) sites are arrayed on a climosequence across Kohala Mountain ranges (Fig. 1). The humid regolith is in the roadcut along Highway 270 (the vicinity of the Bond Estate, N: 20.2288, W: -155.7896), and the arid regolith is situated in another roadcut along the same highway between Mahukona and Kaiwaihae (N: 20.1357, W: -155.8859). We sampled sites on interfluves which in the humid site was flanked by a perennial stream and in the arid site by ephemeral (mostly dry) stream channels. Because regolith is an open chemical and physical system, it could be influenced by weathering of native lava as well as allochthonous addition of minerals and soluble ions. In Hawai'i, atmospheric addition of Asian dust and marine aerosols becomes an important determinant of soil chemistry because primary basaltic materials are nearly depleted through weathering (Kennedy et al.,

1998; Vitousek et al., 1999; Porder et al., 2007; Chadwick et al., 2009). In response to MAP variations, mineralogy, ecology, and geomorphology of the regoliths are quite different, and have been well characterized (e.g., Capo et al., 2000; Whipkey et al. 2002; Goodfellow et al., 2014). Given previous studies have confirmed the contribution of Asian dust to Hawaiian soil cation budgets (Chadwick et al., 1999; Kurtz et al., 2001; Stewart et al., 2001; Porder et al., 2007; Vogel et al. 2021), regolith K of a dust origin needs to be assessed. Previous studies suggested that the average composition of Asian dust added to Hawai'i has not varied since Pliocene (Kyte et al., 1993), and that modern Asian dust largely reflects the average UCC composition (Zieman et al., 1995). Hence, we tentatively used K of the upper continental crust (UCC, Rudnick and Gao, 2013; Huang et al., 2020) to characterize K inputs from a dust source, which is recommended in Kurtz et al. (2001). In the text, we used the term "mineral aerosol" instead of "dust" for long-distance transported solid materials. In Hawai'i, mineral aerosol inputs are positively linked to the substrate age and rainfall (Chadwick et al., 2003).

Based on the vertical transition in chemical composition, texture, color, hardness, and fracture spacing, the outcrop of humid regolith (~15 m in thickness, intensely weathered) could be divided into 13 units (Goodfellow et al., 2014). A sandwiched "corestone zone" between saprolites and soils appears at 3-m depth. The outcrop of arid regolith (~3.5 m in thickness) is divided into 5 units (Goodfellow et al., 2014). A carbonate-enriched layer occurs between 1 and 2-m depth (Capo et al., 2000). We note that both humid and arid regoliths are highly weathered and near-completely depleted of original materials and composed

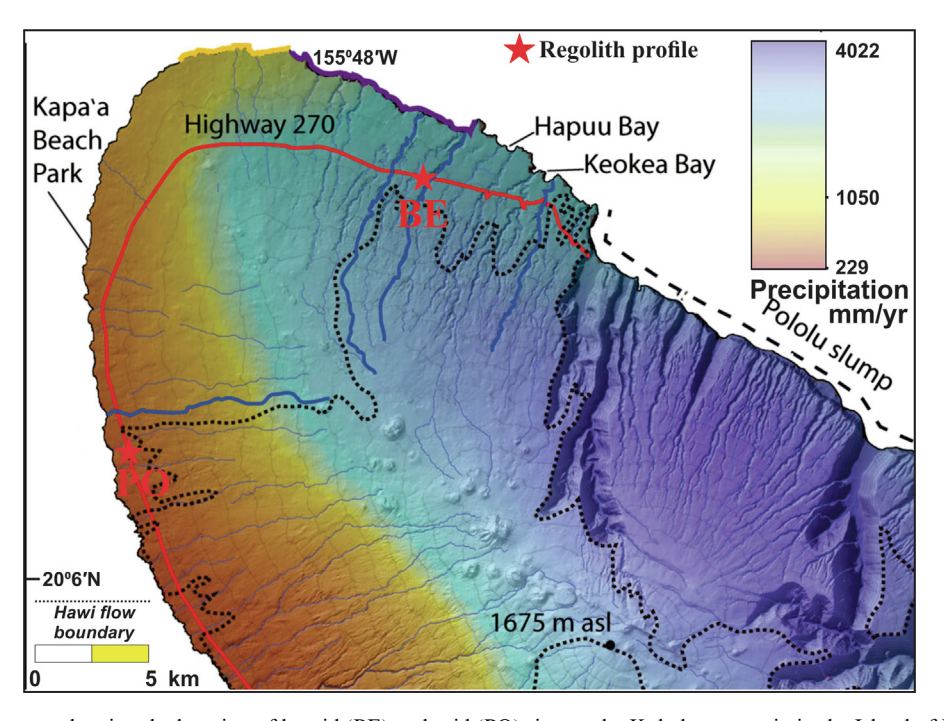


Fig. 1. Geological maps showing the location of humid (BE) and arid (PO) sites at the Kohala mountain in the Island of Hawai'i. Substrate ages were reported in Chadwick et al. (2003), and mean annual precipitation (MAP) was documented in Giambelluca et al. (2013) and the 2011 Rainfall Atlas of Hawai'i by the Department of Geography of the University of Hawai'i at Mänoa.

of secondary clays such as gibbsite, kaolin (kaolinite and halloysite), iron hydroxides, and amorphous intermediates (i.e., short-range-ordered minerals such as allophane) (Goodfellow et al., 2014; Li et al., 2020). The exceptional cases include the corestone (BE14) in the humid regolith and deepest samples of both sites (i.e., 6 m depth, BE16, humid site; 3 m depth, PO10, arid site) with little evidence of weathering except along fractures in the rock. Quartz is absent from the basaltic substrate and its accumulation in Hawaiian soils reflects deposition of mineral aerosols transported from Asia (Kurtz et al., 2001). Quartz accounts for $\sim 10\%$ in the shallow humid regolith and the topmost horizon of the arid regolith. Illite/mica in Hawaiian soils is derived from mineral aerosols (Kurtz et al., 2001; Ziegler et al., 2003), showing marked enrichment in the humid shallow regolith and the surface of the arid regolith (3-4%). The physicochemical property of the regolith is summarized in Supplementary data 2.

Although we have no direct knowledge of anthropogenic additions to the sampling sites, local experts told us that K fertilization was not common on lands similar to the sparsely vegetated arid site or the macademia nut orchard on the humid site. We found no direct evidence of anomalous enrichment of K in soils based on published elemental and radiogenic Sr isotopic compositions in ammonium acetate (NH₄Ac) extracts (i.e., soil exchangeable pools) in Hawai'i (Chadwick et al. 2009; Li et al., 2021c).

Three groups of samples were collected from the field. We sampled the Pololū basalt and Hāwī ash from nearby outcrops to evaluate local sources including parent basalts (Pololū lava) and Hāwī ash that have been incorporated into the older Pololū soils. We sampled \sim 6-m depth for the humid regolith and \sim 3.5-m depth for the arid regolith. For ease of reading, we use "the shallow regolith" to refer to soil horizons ≤ 1 m depth, and "the deep regolith" >1m depth to refer to the deepest saprolitic unit available. A total of 26 regolith samples were collected. Parent basalts and Hāwī ashes were sampled from nearby fresh crops. We collected local rainwater in the years of 2018 and 2019, which was sampled using polyethylene bottles after filtration $< 0.45 \ \mu m$ (cellulose acetate, Thermo ScientificTM) with rapid acidification.

3. ANALYTICAL METHODS

3.1. Chemical extraction

Chemical processes were conducted in a vented laminar flow hood (class-100) (AircleanTM). Samples were processed with double-distilled acids and ultrapure reagents. Exchangeable K was extracted using 1 M ammonium acetate (NH₄Ac) buffered at the pH = 7 for 24 h (Table 1). We note that carbonate materials can be attacked by acetate during leaching (Dohrmann, 2006).

3.2. Element analysis

Element analysis was performed on a Q-ICP-MS (AgilentTM 7900) at the Plasma Mass Spectrometry Laboratory,

the University of North Carolina at Chapel Hill. Homogeneously powdered samples (~100 mg) were transferred into 15 mL Teflon vessels and fully dissolved using a mixture of concentrated HCl + HNO₃ + HF (Li et al., 2019b). Reactors were transferred onto the hotplate over 120 °C until solutions clear (i.e., complete dissolution, five days in general). After drying down, residues were refluxed using 5 mL 2% HNO₃ for analysis. Internal standards of Be, Ge, Rh, In, Ir, and Bi were added for drift correction. Elements including K, Mg, Al, Sr, and Nb, etc. were measured for samples and USGS references (BHVO-2, basalt; GSP-2; granodiorite). External accuracy was <10% (measured data to reported data) (Table S2). The relative gain $(\tau_{K,Nb} > 0)$ and loss ($\tau_{K,Nb} \le 0$) of K in depth were estimated as follows (Brimhall and Dietrich, 1987; Chadwick et al., 1999): $\tau_{j,w} = (C_{j,w} \times C_{i,p})/(C_{j,p} \times C_{i,w}) - 1$, where C denotes the concentration of an element of interest, w and p are weathered and pristine materials (the basalt substrate), respectively, and i and j are the immobile and mobile elements in profiles, respectively. Kurtz et al. (2000) evaluated the mobility of refractory elements in Hawaiian soils and suggested niobium (Nb) is the least mobile element compared to zirconium (Zr), thorium (Th) and hafnium (Hf), etc. Therefore, we used Nb as the immobile element in Hawaiian soils for the calculation of K gain (or loss) in studied regoliths.

3.3. Potassium isotope analysis

An aliquot of each dissolved samples (in 2% HNO₃) was dried down completely and then dissolved in 2 mL 0.7 M HNO₃ for chromatography. The column separation method was reported in Chen et al. (2019). Samples in 0.7 M HNO₃ (100-1000 μg K) were loaded onto the first column (ID of 1.5 cm), containing 17 mL AG50-X8 cation-exchange resin (200–400 mesh, Bio-Rad™). The first step is to separate K from much of the matrix elements (e.g., Na, Mg, and Ca). The first K fraction was collected, evaporated to dryness, and redissolved in 1 mL 0.5 M HNO₃. Samples (in 0.5 M HNO₃) were passed through the second column (ID of 0.5 cm), filled with 2.4 mL AG50-X8 resin (200-400 mesh, Bio-Rad™). The aim of the second step was to separate K from Rb and Cr. We confirm that the yields of studied samples through the column separation were over 99% by monitoring the pre-cuts and post-cuts for both steps of the column chemistry. For all studied samples, we ensured that matrix elements in solution were <2% of K. If collected K fractions (after twostep purification) contained >2% matrix elements (in some cases), a third step was applied to further purify K using the same separation method as the second step. Total procedural blanks were monitored ($\sim 0.1 \mu g$), and in all cases, negligible relative to sample K at mg-levels. Samples were then evaporated to dryness and dissolved in 2% HNO₃.

3.4. Potassium isotope analysis

Potassium isotope analyses were performed using a Nu Plasma II high-resolution MC-ICP-MS at the Isotope Laboratory, University of Washington, Seattle. Isotope analy-

Table 1
Physicochemical and mineralogical characterization of the Hawaiian humid and arid regoliths.

Region	No.	Depth (cm)	pН	OM (%)	C _{org} (%)	Quartz (%)	Illite/mica (%)	Total K (mg·g ⁻¹)	$K_{\mathrm{NH4Ac}} \ (\mathrm{mg} \cdot \mathrm{g}^{-1})$	K/Al molar ratio	$ au_{K,Nb}$
Humid (BE)	BE1	2.5	5.6	21.5	10.18	9	2.7	18.7	0.2	0.09	0.93
MAP = $1730 \pm 57 \text{ mm} \cdot \text{a}^{-1}$	BE2	17.5	5.7	6.5	2.77	11	2.8	30.1	0.3	0.09	0.45
	BE3	33.5	5.4	3.0	2.22	10	3.0	15.3	0.1	0.09	-0.34
	BE4	46	5.6	2.9	2.07	11	3.0	11.1	0.2	0.06	-0.32
	BE5	61	5.8	1.8	1.06	11	2.8	11.8	0.2	0.06	-0.03
	BE6	96.5	5.9	2.7	1.06	2	3.1	4.5	0.1	0.08	-0.70
	BE7	127	6.0	2.7	0.99	0	2.8	7.7	0.1	0.04	-0.50
	BE8	158.5	6.1	3.5	1.03	0	2.4	7.9	0.1	0.04	-0.44
	BE9	192	6.2	3.3	0.73	0	2.4	2.8	0.1	0.01	-0.64
	BE10	230	6.3	1.7	0.6	0	0.9	1.4	0.1	0.01	-0.80
	BE11	259	6.4	4.3	0.38	0	0.9	1.3	0.0	0.01	-0.91
	BE12	297.5	6.2	2.0	0.28	0	0.8	0.7	0.1	0.00	-0.96
	BE13	300	n.d.	n.d.	n.d.	0	0.4	0.8	0.1	0.01	-0.84
	BE14	300	n.d.	n.d.	n.d.	n.d.	n.d.	4.2	0.4	0.05	-0.16
	BE15	337.5	5.7	1.0	0.06	n.d.	n.d.	0.4	n.d.	0.00	-0.97
	BE16	600	n.d.	n.d.	n.d.	n.d.	n.d.	4.8	n.d.	0.06	-0.04
Arid (BE)	PO1	2.5	7.9	11.0	2.5	11	3.6	0.9	0.2	0.03	-0.85
$MAP = 385 \pm 53 \text{ mm} \cdot \text{a}^{-1}$	PO2	17.5	7.7	2.8	1.3	0	3.7	1.9	0.2	0.02	-0.81
	PO3	34.5	7.7	2.4	1.8	0	1.2	0.8	0.1	0.00	-0.90
	PO4	51.5	8.3	2.2	0.9	0	0.7	1.2	0.2	0.00	-0.87
	PO5	70	8.7	3.4	0.9	0	0.9	2.1	0.3	0.01	-0.75
	PO6	75	8.6	3.0	0.8	0	1.1	2.0	0.2	0.01	-0.74
	PO7	96	8.6	3.6	0.7	0	1.6	3.0	0.3	0.01	-0.61
	PO8	108.5	8.5	1.6	0.5	0	0	1.1	0.1	0.01	-0.87
	PO9	200	n.d.	n.d.	n.d.	n.d.	n.d.	0.4	0.1	0.01	-0.90
	PO10	300	n.d.	n.d.	n.d.	n.d.	n.d.	8.8	0.1	0.08	0.00
Ash	Hāwī	n.d.	n.d.	n.d.	n.d.	n.d.	n.d.	n.d.	n.d.	0.05	n.d.
Bedrock	Pololū	n.d.	n.d.	n.d.	n.d.	n.d.	n.d.	8.1	n.d.	0.05	0.00

Note 1. n.d.: not determined. OM: soil organic matter content. C_{org} : organic carbon content; $\tau_{K,Nb}$ represents K mass transfer coefficient, which is indexed to an immobile element (i.e., Nb, Kurtz et al., 2000).

Note 2. Mineralogical data are from Li et al. (2020).

ses were conducted in the "cold plasma" mode (i.e., the RF forward power ranging from 750 to 850 W) using a DSN-100 desolvation system, with a PFA spray chamber and a C-Flow PFA microconcentric nebulizer. The residual ⁴⁰Ar¹H⁺ beam as resolved from ⁴¹K⁺ using pseudo-high resolution mode (high-resolution: >10,000), providing interference-free shoulders of ³⁹K⁺ and ⁴¹K⁺ for isotopic measurements. The analytical sensitivity was 2.8 V/ppm, and the on-peak zero was ${}^{41}\text{K}$: $-2.7 \cdot 10 \text{(BE)}$ MAP = 1730 \pm 57 mm·a⁻³; ³⁹K: 6.9·10(BE) MAP = 1730 \pm 57 mm·a⁻⁴. Each analysis represents an average of 50 cycles of 5 s onpeak integrations. A blank was measured at the beginning of each sample-standard analysis and was subtracted from measured ion beams. The K isotope ratios were measured using a sample-standard bracketing protocol (6–8 cycles for each sample). For further information on Instrumentation and analytical methods see Hu et al. (2018) and Xu et al. (2019). The isotopic composition was expressed in per mil (%) using a delta notation relative to the NIST SRM 3141a standard:

$$\delta^{41}K(\%e) = \left\{ \frac{({}^{41}K/{}^{39}K)_{sample}}{({}^{41}K/{}^{39}K)_{NIST SRM 3141a}} - 1 \right\} \times 1000 \tag{1}$$

Two standard deviations (2 S.D.) and 95% confidence interval (95% c.i.) were provided in Table S3 and we reported 2 S.D. values in the text and plots. USGS references BHVO-2 yields $\delta^{41}K$ of $-0.49\pm0.10\%$ and $-0.48\pm0.07\%$, and GSP-2 yields $\delta^{41}K$ of $-0.46\pm0.09\%$ and $-0.43\pm0.07\%$, which are in line with inter-laboratory comparison (Table S3). We use a notation $\Delta^{41}K_{x-y}$ equal to $\delta^{41}K_x$ - $\delta^{41}K_y$ to express isotope fractionation between the components \times and y. We note that confidence intervals (95% c.i.) were used to reflect statistical clarity of data from each sample, calculated as:

95% c.i. (‰) =
$$t_{n-1} \times \frac{S.D.}{\sqrt{n}}$$
, (2)

where S.D. denotes the standard deviation over analytical sessions (n times) of samples, and t_{n-1} denotes student's law factor with (n-1) degrees of freedom at a 95% confidence level (Table 2).

3.5. Radiogenic Nd-Sr isotopes

All pretreatment and measurement were performed at the State Key Laboratory of Marine Geology, Tongji University. About 50 mg powders were digested for Sr and Nd isotopic analysis. The aliquots were dried, treated three times with 1 mL conc. HNO₃ at 110 °C, and equilibrated in 2.5 M HCl. The samples were then loaded in 2.5 M HCl on 1 mL AG 50 W-X8 (200–400 mesh) cation-exchange resin for the separation of strontium and the REEs. The Nd fraction was further separated from the REE using ion-exchange columns filled with Ln Spec resin. Radiogenic Sr-Nd isotopes were measured on a Thermo-Finnigan Neptune Plus MC-ICP MS.

The $^{87}\text{Sr}/^{86}\text{Sr}$ ratio was monitored using SRM987 standard (0.710248) for detector efficiency drift and normalization, yielding an $^{87}\text{Sr}/^{86}\text{Sr}$ ratio of 0.710271 \pm 18 (2 S.D.). For Sr analyses, the internal mass fractionation was

corrected, assuming an $^{86}\text{Sr}/^{88}\text{Sr}$ ratio of 0.1194 (Nier, 1938) and using the exponential law. Minor interferences of ^{87}Rb on ^{87}Sr were corrected by $^{85}\text{Rb}/^{87}\text{Rb}$ of 2.59265. The Nd isotopes mass bias was normalized to $^{146}\text{Nd}/^{144}\text{Nd}$ of 0.7219. The isotopic value was expressed as ϵ Nd, equal to $[(^{143}\text{Nd}/^{144}\text{Nd})_{\text{Measured}}/(^{143}\text{Nd}/^{144}\text{Nd})_{\text{CHUR}} - 1] \times 10^4$, in which a CHUR (chondritic uniform reservoir) ratio is 0.512638.

USGS references BHVO-2 and BCR-2 (basalts) were comparably monitored during this study. The measurement of BHVO-2 yields ¹⁴³Nd/¹⁴⁴Nd and ⁸⁷Sr/⁸⁶Sr of 0.512987 and 0.703506, respectively. Measurements of BCR-2 yield ¹⁴³Nd/¹⁴⁴Nd of 0.512655 and ⁸⁷Sr/⁸⁶Sr of 0.705064. Total blanks < 100 pg Sr and 30 pg Nd are negligible relative to Nd and Sr mass in regolith samples. Regolith samples and the basaltic substrate (the Pololū lava and Hāwī ash) were measured for Nd and Sr isotopic composition. Only some samples of the deep regolith were measured for εNd and ⁸⁷Sr/⁸⁶Sr because we suspected (and confirmed) that isotope ratios in the deeper samples would represent rock-derived values. One rainwater sample was analyzed for ⁸⁷Sr/⁸⁶Sr (Table 2).

4. RESULTS

4.1. K element composition of the bulk and extracted fractions

The humid regolith shows an upward increase in [K] (0.4–30.1 mg·g⁻¹, Fig. 2a), whereas [K] in the arid regolith is depleted relative to unweathered basalt and varies little with depth (0.4–3.0 mg·g⁻¹, Fig. 2a). In the deepest samples (6-m in the humid site, 3-m in the arid site), [K] is close to the basaltic composition. In the humid regolith, τ_{K,Nb} ranges from -0.97 to 0.93 with the positive values near the surface suggesting addition of K from an external source (Fig. 2b). Local-scale K enrichment is marked at the top (<20 cm, $\tau_{K.Nb}$ of 0.45–0.93). In the deep, humid regolith, the corestone zone and the bottom layer exhibits minimal K depletion ($\tau_{K,Nb}$ from -0.16 to -0.04). Across the arid regolith, there is an overall depletion of K supported by $\tau_{K,Nb}$ from -0.90 to -0.61, except for the deepest horizon chemically close to the basaltic substrate $(\tau_{K,Nb} = 0)$. Exchangeable K extracted using NH₄Ac in the humid regolith ranges from 0 to 0.4 mg·g⁻¹, making up only 0 to 9.5% total K (Table 1). In contrast, exchangeable K in the arid regolith makes up a more substantial portion of the total pool (1.1 to $\sim 35\%$, 0.1–0.6 mg·g⁻¹), particularly significant at the carbonate layer where the extraction may be releasing solid phase K (Fig. 2c).

4.2. K isotope composition of the bulk and extracted fractions

The humid regolith shows $\delta^{41}K$ ranging from -0.76 ± 0.08 to $-0.31 \pm 0.06\%$ (Fig. 3a). This range is relatively narrow in the shallow regolith (-0.62 ± 0.03 to $-0.49 \pm 0.06\%$, Fig. 3a), values that are close to, but slightly more negative than those of the Pololū basalt ($-0.48 \pm 0.06\%$) and Hāwī ash ($-0.48 \pm 0.10\%$). In deep, humid regolith, samples in 1–2 m have $\delta^{41}K$ slightly heavier

Table 2 Isotopic compositions of Hawaiian humid and arid regoliths.

Region	No.	Depth (cm)	δ ⁴¹ Κ	95% c.i. (‰)	2 S.D. (‰)	N	εNd	⁸⁷ Sr/ ⁸⁶ Sr
		,	(‰)					
Humid (BE)	BE1	2.5	-0.49	0.04	0.06	7	-8.15	0.71941
$MAP = 1730 \pm 57 \text{ mm} \cdot \text{a}^{-1}$	BE2	17.5	-0.54	0.05	0.07	7	-7.79	0.71811
	*BE2		-0.63	0.05	0.07	8	n.d.	n.d.
	BE3	33.5	-0.62	0.05	0.06	6	-7.92	0.72233
	*BE3		-0.35	0.05	0.07	7	n.d.	n.d.
	BE4	46	-0.51	0.04	0.09	7	-7.20	0.72129
	BE5	61	-0.55	0.05	0.09	6	-6.60	0.72177
	BE6	96.5	-0.49	0.04	0.06	6	-5.43	0.71814
	*BE6		-0.23	0.06	0.07	7	n.d.	n.d.
	BE7	127	-0.44	0.05	0.07	6	-4.40	0.71549
	BE8	158.5	-0.42	0.04	0.07	7	-1.89	0.70375
	BE9	192	-0.53	0.05	0.08	6	n.d.	n.d.
	BE10	230	-0.42	0.05	0.08	6	n.d.	n.d.
	BE11	259	-0.63	0.05	0.05	6	n.d.	n.d.
	BE12	297.5	-0.72	0.04	0.05	6	n.d.	n.d.
	*BE12		-0.19	0.07	0.10	8	n.d.	n.d.
	BE13	300	-0.31	0.05	0.06	6	-0.14	0.70385
	BE14	300	-0.52	0.04	0.04	7	n.d.	n.d.
	BE15	337.5	-0.76	0.05	0.08	6	n.d.	n.d.
	BE16	600	-0.50	0.04	0.06	8	4.40	0.70396
Arid (BE)	PO1	2.5	-0.25	0.05	0.06	7	-0.29	0.70613
$MAP = 385 \pm 53 \text{ mm} \cdot \text{a}^{-1}$	PO2	17.5	-0.03	0.04	0.05	6	3.80	0.70575
	*PO2		0.04	0.06	0.08	9	n.d.	n.d.
	PO3	34.5	-0.37	0.08	0.06	6	4.78	0.70554
	PO4	51.5	-0.43	0.05	0.11	7	6.66	0.70533
	PO5	70	-0.23	0.05	0.08	4	6.62	0.70573
	*PO5		-0.01	0.04	0.05	8	n.d.	n.d.
	PO6	75	-0.34	0.04	0.05	6	6.45	0.70523
	PO7	96	-0.37	0.04	0.06	7	6.58	0.70534
	PO8	108.5	-0.37	0.04	0.07	6	6.70	0.70331
	PO9	200	-0.02	0.04	0.06	6	n.d.	0.70735
	*PO9		0.03	0.05	0.07	7	n.d.	n.d.
	PO10	300	-0.39	0.04	0.10	6	5.12	0.70367
Rainwater	R1	n.d.	-0.21	0.09	0.11	7	n.d.	0.71056
	R2	n.d.	-0.16	0.04	0.07	7	n.d.	n.d.
Ash	Hāwī	n.d.	-0.48	0.08	0.10	7	n.d.	0.70423
Bedrock	Pololū	n.d.	-0.48	0.04	0.06	6	6.93	0.70377

Note 1. 95% c.i. = 95% confidence interval, which denotes the two standard error corrected by the Student's t factor (Hu et al., 2018); 2 S.D. denotes the two standard deviation.

Note 2. The certified SRM 987 value = 0.710248 is used for normalization. Measured mean SRM 987 value is 0.710271 ± 18 (2 S.D.).

Note 3. *NH₄Ac extraction of bulk regolith samples.

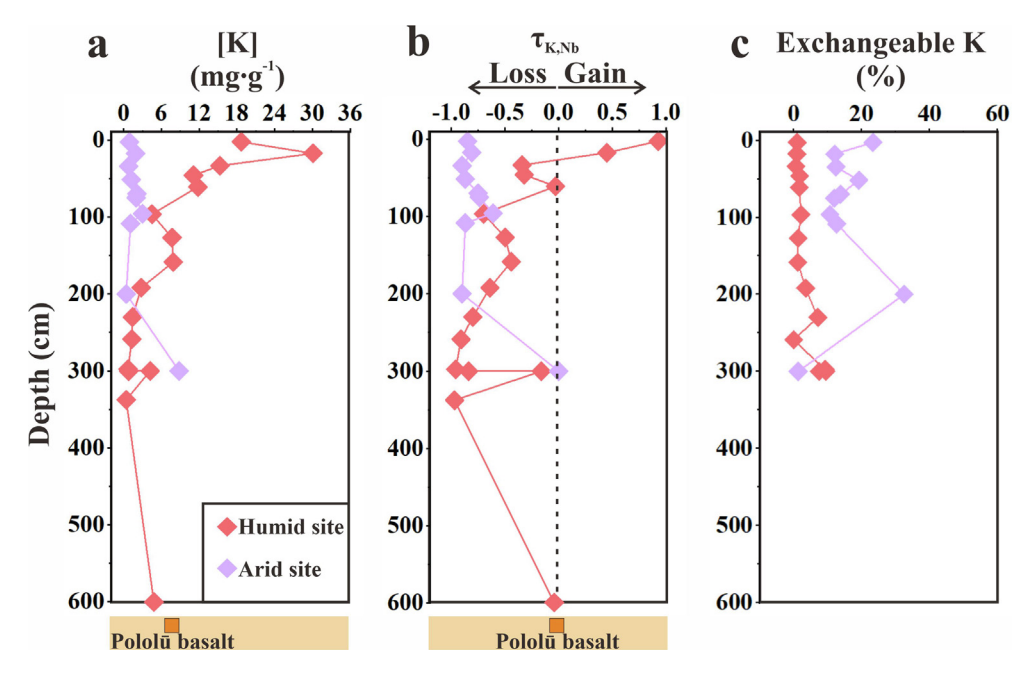


Fig. 2. Vertical distribution of (a) [K] (K concentration), (b) $\tau_{K,Nb}$ (K mass transfer coefficient), and (c) the fraction (%) of K that is in a exchangeable form (NH₄Ac-K) in the humid and arid regoliths. The composition of the basalt substrate is shown at the bottom (Data tabulated in Table 1 and supplementary data 2).

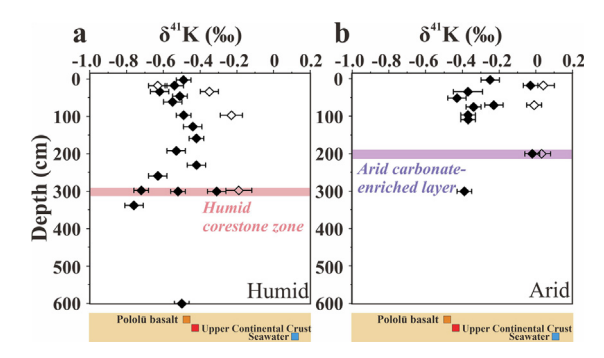


Fig. 3. Vertical distribution of $\delta^{41}K$ values (isotopic composition) in the (a) humid and (b) arid regoliths. Bulk and NH₄Ac extraction samples are symbolized using solid and hollow diamonds, respectively. The $\delta^{41}K$ data of the basalt substrate (this study), the upper continental crust (UCC, Huang et al., 2020), and the modern seawater (Hille et al., 2019; Wang et al., 2020) are shown at the bottom. The corestone zone in the humid site and the carbonate-enriched layer in the arid site are highlighted using pink and purple bars, respectively (Data tabulated in Table 2 and supplementary data 2).

or similar to that of the basalt, and samples in deeper sites exhibit $\delta^{41}K$ more negative than basaltic $\delta^{41}K$. We note that the corestone sample at 300 cm depth has $\delta^{41}K$ (-0.5 $2 \pm 0.04\%$) close to basaltic $\delta^{41}K$. The arid regolith displays $\delta^{41}K$ ranging from -0.43 \pm 0.11 to -0.02 \pm 0.06%, primarily higher than that of the basaltic substrate and the range reported for weathering profiles (Chen et al., 2019; Teng et al., 2020) (Fig. 3b). We note that the carbonate-enriched zone (100–200 cm depth) has an enriched isotopic value of -0.02 \pm 0.06% (PO9, 200 cm

depth), which is similar to the subsurface soil (PO2, $-0.03 \pm 0.05\%$, Table 2). Collected rainwaters have $\delta^{41}K$ values from $-0.21 \pm 0.11\%$ to $-0.16 \pm 0.07\%$.

For the most part, exchangeable K has $\delta^{41}K$ that are more positive than the corresponding bulk values. Exchangeable K (NH₄Ac-K) of the humid profile has $\delta^{41}K$ values from -0.63 ± 0.07 to $-0.35 \pm 0.07\%$. Exchangeable K of BE2 (17.5 cm) has lower $\delta^{41}K$ ($-0.63 \pm 0.07\%$) than the bulk ($-0.49 \pm 0.06\%$). Exchangeable K of samples from the deeper horizons has higher $\delta^{41}K$ than their bulk values. In comparison, exchangeable K of the arid profile exhibits $\delta^{41}K$ from -0.01 ± 0.05 to $0.04 \pm 0.08\%$. The exchangeable K of PO5 exhibits $\delta^{41}K$ higher than its corresponding bulk value. The exchangeable K of PO2 and PO9 exhibits $\delta^{41}K$ similar to corresponding bulk values.

4.3. Nd and Sr isotope compositions

The humid regolith has ⁸⁷Sr/⁸⁶Sr ranging from 0.70375 to 0.72233 and the arid regolith has ⁸⁷Sr/⁸⁶Sr ranging from 0.70367 to 0.72613, including ⁸⁷Sr/⁸⁶Sr data from Li et al. (2020) (Table 2). The humid regolith has εNd ranging from -8.15 to 4.40, whereas the arid regolith has εNd ranging from -0.29 to 6.70 (Table 2). The Pololū basalt has εNd and ⁸⁷Sr/⁸⁶Sr of 6.93 and 0.70377, respectively (Table 2). The Hāwī ash has ⁸⁷Sr/⁸⁶Sr of 0.70423 and the rainwater sample has ⁸⁷Sr/⁸⁶Sr of 0.71056. The εNd values in both regoliths become less radiogenic toward the surface (humid: from 4.4 to -8.15; arid: from 5.12 to -0.29), while ⁸⁷Sr/⁸⁶Sr values increase toward the surface (humid: from 0.70396 to 0.72233; arid: from 0. 70,735 to 0.70523). In particular, the humid regolith shows lower εNd and higher ⁸⁷Sr/⁸⁶Sr values compared to the arid regolith. The Nd isotope

systematics can provide quantitative estimate of the mass of mineral aerosols added based on a mass-balance method (equations 4–6 in Kurtz et al., 2001). Using εNd-based mass balance (Kurtz et al., 2001), accumulation of mineral aerosols within each horizon accounts for 42–89% (humid) and 2–43% mass (arid). The mineral aerosols deposition rates (taken as conservative estimates) are 4.3 t·km⁻²·yr⁻¹ (humid) and 0.3 t·km⁻²·yr⁻¹ (arid) (Table 3).

5. DISCUSSION

The K isotope compositions of two regoliths display significant variations, reflecting isotopic fractionation regulated by different geological processes. From the comparison of $\tau_{K,Nb}$ (an index of K gains/losses) versus $\delta^{41}K$ (Fig. 4a), we found three directions of element-to-isotope covariations revealing that at least three controls act to modulate the $\delta^{41}K$ composition. In the humid, shallow regolith, two samples display K enrichment (relative to the parent rock) and basalt $\delta^{41}K$. For most samples of the humid regolith, $\delta^{41}K$ decreases with progressive K depletion. In contrast, $\delta^{41}K$ in most samples of the arid regolith increases with K loss. Here, we summarize three possible factors contributing to $\delta^{41}K$ variations in the regolith, including atmospheric addition, clay formation, and plant cycling.

5.1. Atmospheric addition

As regolith develops, atmospheric addition becomes increasingly important in modulating its mineralogy and chemistry (Chadwick et al., 2009; Goodfellow et al., 2014). There are two major atmospheric sources regulating regolith $\delta^{41}K$ composition in the study area, namely mineral and marine aerosols.

Globally transported dusts accumulate in Hawaiian soils, which potentially play an important role in determining bulk elemental and isotopic composition of the regolith (Kurtz et al., 2001; Ziegler et al., 2003; Wiegand et al., 2005; Derry and Chadwick, 2007; Ryu et al., 2014; Li et al., 2020). The contribution from mineral and marine aerosols to the regolith cation budget positively correlates to rainfall (Porder et al., 2007). Previous work documented that the average composition of Asian dusts delivered to Hawai'i remains near-constant since the Pliocene (Kyte et al., 1993), and that modern Asian dusts primarily reflect the average UCC composition (Zieman et al., 1995). Therefore, mineral aerosolrelated features can be easily identified in the humid regolith, which exhibit near-homogeneous δ^{41} K (\sim -0.6 to -0.5%) identical to (or slightly lower than) those of the UCC (ave. -0.44%, Huang et al., 2020). First, there is an upward reduction in the degree of K loss (i.e., an increase in $\tau_{K,Nb}$) in humid, shallow regolith (Table 1), with the maximum $\tau_{K,Nb}$ up to 0.93 (i.e., K enrichment) at the surface (BE1 and BE2). This pattern is contrary to typical depletion profiles which show greatest loss in the surface and near-surface horizons and can be explained by the deposition of mineral aerosols that may balance or even overwhelm the leaching loss of soluble ions like K+ during weathering (Chadwick et al., 1999). Using the average UCC composition (Rudnick and Gao, 2013) as an analogue of mineral aerosols added onto Hawaiian soils (Kurtz et al., 2001), the K/Nb ratio in mineral aerosols (1.88 mg/μg) is higher than the basaltic parent (0.35 mg/µg). Therefore, the deposition of mineral aerosols could cause the enrichment of K ($\tau_{K,Nb} > 0$) and UCC-like δ^{41} K signals (Fig. 4a). Second, there is a linkage between the δ^{41} K of bulk regolith samples and the content of quartz (Fig. 4b). In Fig. 4b, humid, shallow regolith and the arid top-most soil exhibit narrower δ^{41} K variations and higher quartz contents (~10-12%) compared with corresponding lower horizons, reflecting the contribution of accreted Asian dusts (δ^{41} K_{UCC}, Huang et al., 2020; quartz: 20%, Kurtz et al., 2001). Following the method in Kurtz et al. (2001), we calculated mineral aerosols fluxes of 4.3 and 0.3 t·km⁻²·yr⁻¹ for the humid and arid sites using ENd, respectively (Table 3). It supports the conclusion of substantial dust imprints on the humid regolith relative to the arid regolith based on soil mineralogy (e.g., the enrichment of quartz).

Regolith profiles in near-coastal settings are influenced by the deposition of marine aerosols, modulating the K isotope composition of bulk samples and their extraction. First, the arid regolith has δ^{41} K (-0.43 to -0.02%) higher than the basaltic composition (-0.48%), which can be partially attributed to seawater K imprint (~0.14%, Hille et al., 2019; Wang et al., 2020). In the arid regolith, seawater-derived K may be better preserved than the humid regolith without marked leaching loss because of high evapotranspiration over precipitation (Goodfellow et al., 2014). The carbonate-enriched layer of the arid regolith has an ⁸⁷Sr/⁸⁶Sr value of 0.70735, likely representing a mixture of basalt-derived Sr (\sim 31%, Pololū basalt, 0.70377) and seawater/rainwater-derived Sr (~69%, modern seawater 0.709, Table S4) based on isotope mixing. The carbonateenriched layer has the highest δ^{41} K value of -0.02%, which is close to modern seawater δ^{41} K ($\sim 0.14\%$, Wang et al., 2020) compared with the rest samples. We infer that seawater K may be partially retained in pedogenetic carbonates (e.g., dolomite, Capo et al., 2000) (or other evaporitic deposits) in the arid regolith, because carbonates can be partially extracted using NH₄Ac (Dohrmann, 2006). The carbonate-enriched layer exhibits the highest exchangeable K fraction within the profile ($\sim 35\%$) (Table 1). Second, NH_4Ac extraction (exchangeable K) has $\delta^{41}K_{NH4Ac}$ values higher than corresponding bulk values for both regoliths (except for one humid, subsurface sample BE2, 17.5 cm) (Fig. 3). It is expected because porewater may receive higher K contribution from marine aerosols compared to the bulk samples and commonly reflects a mixing between basaltic and seawater sources. In the humid site, there is an increase in $\delta^{41}K_{NH4Ac}$ with depth (Fig. 3), which may be explained by the replenishment of K of a seawater origin in near-marine environments and the "leakiness" of K via precipitation infiltration. We note that local rainwater samples have δ^{41} K from -0.21 to -0.16% and 87 Sr/ 86 Sr of 0.71059 (close to seawater values of \sim 0.709, Table S4). In addition, there is a good correspondence between

Table 3 Calculated eolian inputs by ϵNd in Hawaiian humid and arid regoliths.

Region	Sample	Depth (cm)	Density (g/cm ⁻³)	εNd	Mineral aerosol (wt.%)	Mass Mineral aerosols (t/km²)	Flux aerosols (t/km²/yr)
Humid (BE)	BE1	2.5	1.24	-8.15	89	110,506	4.3
MAP = $1730 \pm 57 \text{ mm} \cdot \text{a}^{-1}$	BE2	17.5	1.26	-7.79	87	186,354	
	BE3	33.5	1.32	-7.92	88	150,604	
	BE4	46	1.17	-7.20	84	117,275	
	BE5	61	1.28	-6.60	80	204,800	
	BE6	96.5	1.62	-5.43	73	142,141	
	BE7	127	1.36	-4.40	67	228,000	
	BE8	158.5	1.32	-1.89	52	248,502	
	BE9	192	1.19	n.d.	n.d.	n.d.	
	BE10	230	1.1	n.d.	n.d.	n.d.	
	BE11	259	1.12	n.d.	n.d.	n.d.	
	BE12	297.5	1.14	-0.14	42	105,336	
	BE13	300	n.d.	n.d.	n.d.	n.d.	
	BE14	300	n.d.	n.d.	n.d.	n.d.	
	BE15	337.5	1.22	n.d.	n.d.	n.d.	
	BE16	600	n.d.	4.40	12	n.d.	
Arid (BE)	PO1	2.5	0.78	-0.29	43	22,195	0.3
$MAP = 385 \pm 53 \text{ mm} \cdot \text{a}^{-1}$	PO2	17.5	1.03	3.80	19	133,362	
	PO3	34.5	0.94	4.78	13	94,387	
	PO4	51.5	1.04	6.66	2	67,741	
	PO5	70	1.04	6.62	2	77,681	
	PO6	75	0.99	6.45	n.d.	n.d.	
	PO7	96	0.97	6.58	2	51,978	
	PO8	108.5	0.85	6.70	2	52,083	
	PO9	200	n.d.	n.d.	n.d.	n.d.	
	PO10	300	n.d.	5.12	1	n.d.	
Bedrock	Pololū	n.d.	1.25	6.93	0	0	

Note 1. We arrive at a long-term rate of mineral aerosol addition by dividing its mass by the age of the Pololū lava (350 kyr, Goodfellow et al., 2014). Nd isotopes provide quantitative estimate of the mass of mineral aerosols based on a mass-balance method (Kurtz et al., 2001).

Note 2. Mineral aerosol fluxes provided represent a conservative estimate because the estimation of BE9, BE10, BE11, BE13, BE14, BE 15 and BE 16 in the humid, deep regolith and PO6, PO9 and PO10 in the arid, deep regolith are not included due to a lack of εNd and/or density data for calculation.

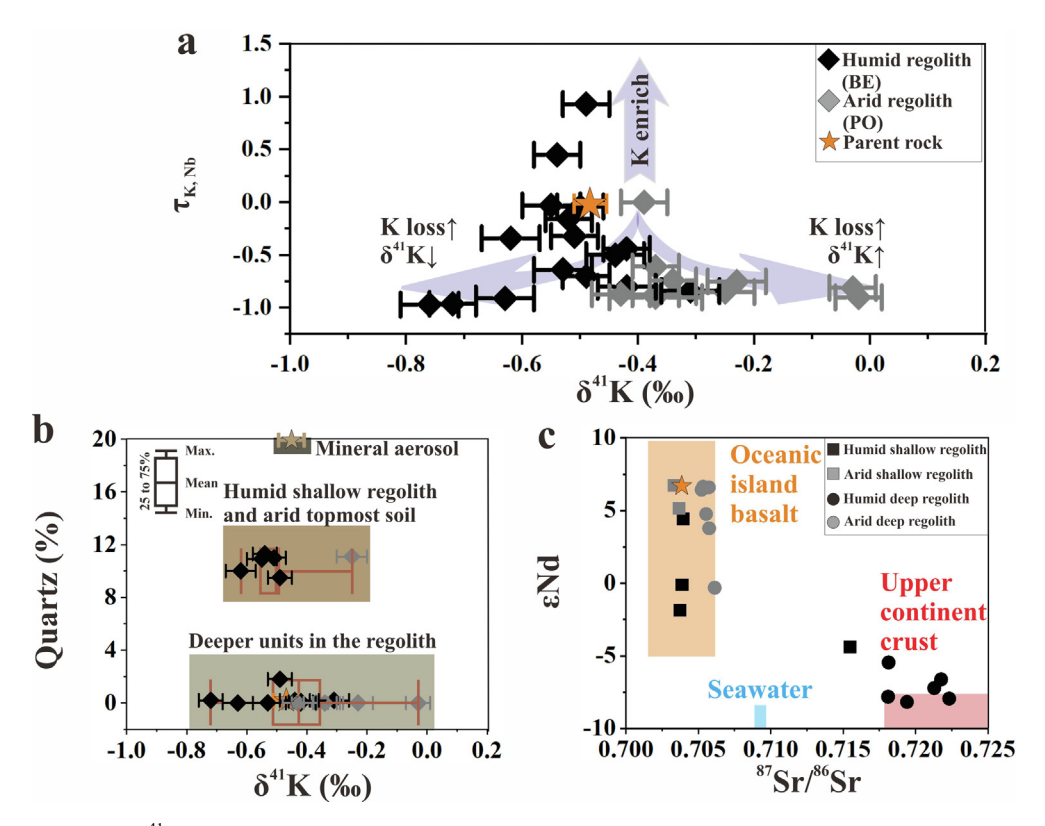


Fig. 4. Interrelationship of $\delta^{41}K$ with (a) $\tau_{K,Nb}$ (the mass transfer coefficient of K), and (b) quartz content (Table 1). In plots (a–b), the data of the humid and arid regoliths are symbolized using black and grey diamonds (95% c.i. uncertainty), respectively. In plot (a), purple arrows indicate K enrichment and two opposite isotopic fractionation trends with K loss. In plot (b), the composition of mineral aerosols is provided by Kurtz et al. (2001) (Asian dust, quartz content: 20%) and Huang et al. (2020) ($\delta^{41}K_{UCC}$: 0.44 \pm 0.05‰). (c) Bulk $^{87}Sr/^{86}Sr$ versus ϵNd data. The Nd and Sr isotope composition ranges of the upper continental crust (UCC), oceanic island basalt and Pacific Ocean seawater are displayed for comparison (Table S4). The Data of the Pololū basalt are marked using an orange star, and data of shallow and regolith regoliths are symbolized by boxes and circles, respectively. (Data tabulated in Tables 1–2 and supplementary data 2).

 $\delta^{41}K_{NH4Ac}$ in the humid, deep regolith (-0.19%) and local rainwater $\delta^{41}K_{.}$ It reveals that marine aerosols K could be introduced to the humid regolith and leached downwards within the profile.

Numerous studies have suggested that radiogenic Nd and Sr isotopes are powerful tools for tracing and quantifying contributions of atmospheric and native materials in Hawaiian soils (e.g., Chadwick et al., 1999; Kurtz et al., 2001), and we tested this idea in this study. It is known that mineral aerosols fluxes corresponding to local rainfall, consistent with the suggestion of upper atmosphere transport and deposition of dust as condensation nuclei in raindrops (Parrington et al., 1983). The estimate of mineral aerosols fluxes at the arid site (MAP: $385 \pm 53 \text{ mm} \cdot \text{yr}^{-1}$) agrees well with the calculation for Hawaiian soils of similar MAP (0.25 to 0.50 t·km⁻²·yr⁻¹) using quartz and mica/illite contents (Porder et al., 2007). However, the estimation of the humid site (MAP of 1730 \pm 57 mm·yr⁻¹) is much higher than the calculation based on quantification using ENd data, quartz and mica/illite content in Hawaiian soils $(1500-2500 \text{ mm}\cdot\text{yr}^{-1}, 1-1.25 \text{ t}\cdot\text{km}^{-2}\cdot\text{yr}^{-1}; \text{ Kurtz et al.},$ 2001; Porder et al., 2007). We infer that this mismatch is possible because our humid site is minimally sloping, and thus unlikely to be losing surface soils by soil creep and wind erosion that could be rich in dust-derived minerals. Alternatively, mica/illite may transform into other clays that were not ascribed to mineral aerosols, causing bias because the calculation assumes that mica/illite in the regolith has not weathered after deposition (Kurtz et al., 2001). Such bias is possible because dust sampled in ship-board measurements near Hawai'i contains ~20% quartz and 30–50% mica/illite (Leinen et al., 1994), and previous Hawaiian soil studies found that soils could contain 30% (quartz + mica/illite) (Porder et al., 2007), and 20% quartz and 10% mica (Kurtz et al., 2001).

The cross-plot of bulk ⁸⁷Sr/⁸⁶Sr and εNd may provide insights into the contribution of major sources (basalts, mineral aerosols, and seawater, Fig. 4c). For example, humid, shallow regolith is featured by UCC signals, in accord with enriched quartz. This dust imprint is also supported by the Nd-Sr similarity to the top of LL44-GPC3 core (⁸⁷Sr/⁸⁶Sr of ~0.717–0.720; εNd of ~-11 to -9.5, Nakai et al., 1993; Pettke et al., 2002; Zhang et al., 2016), which reflects the constant, average composition of Asian dusts delivered to Hawai'i since Pliocene (Kyte et al., 1993). However, seawater K imprint could be easily identified at the arid regolith (Fig. 3), but seawater Nd and Sr signals can be hardly distinguished (Fig. 4c). We suggest that

seawater K cannot be tracked by Nd-Sr isotopes because marine aerosols exert a stronger control on regolith K budget relative to Nd (or Sr) (K/Sr = 48, K/Nd \sim 50,000), compared with mineral aerosols (K/Sr = 33, K/Nd = 860) (i.e., UCC, Rudnick and Gao, 2013) and the basalt (K/Sr = 16, K/Nd = 254). In sum, Nd and Sr isotopes do not capture the full suite of contributions to the weathering profiles in Hawai'i.

5.2. Chemical weathering and clay formation

Based on studies on K isotopes in weathering profiles, the prevalence of negative K isotope shift from basaltic δ^{41} K commonly reflects a mixing between isotopically lighter clays and heavier parent materials (Chen et al., 2019; Teng et al., 2020). We consider that structural incorporation and adsorption (i.e., two dominant ion exchange processes during clay formation, Hindshaw et al., 2019) may be responsible for distinct isotopic compositions in the two profiles (Fig. 3).

Preferential retention of isotopically light K in the humid, deep regoliths agrees with reported patterns of K isotope fractionation during chemical weathering (Fig. 3). It has been well recognized that clay minerals are the major sink of K released from the basaltic substrate during chemical weathering, preferentially taking up isotopically lighter K (S. Li et al., 2019; Chen et al., 2019; Huang et al., 2020; Teng et al., 2020), and releasing heavier K into river water (S. Li et al., 2019; Wang et al., 2021; X. Li et al., 2022). This type of weathering-driven fractionation may cause the positive correlation between bulk δ^{41} K and K/Al ratio (a widely used proxy of weathering intensity, Hu et al., 2016; K is highly mobile relative to Al) (Fig. 5a). In comparison, the humid, shallow regolith samples do not follow this relationship (Fig. 5a) presumably due to the overprinting effect of mineral aerosols, as supported by UCC-like δ^{41} K and high K/Al values $(K/Al_{UCC} \sim 0.28$ and $K/Al_{Basalt} \sim 0.05)$. However, in contrast to previous studies of weathering profiles (Chen et al., 2019; Teng et al., 2020), the arid regolith has higher $\delta^{41}K$ values compared to its basaltic substrate (Fig. 3), implying that clay ³⁹K uptake is not the primary control in this environment. Moreover, there is no distinguishable correlation between bulk δ^{41} K and K/Al values in the arid regolith (Fig. 5a). A possible explanation was provided by a laboratory study of Li et al. (2021a) that the exchangeable complex with K⁺ adsorbed on phyllosilicates, was isotopically heavier than residual K⁺ in water. Using series of sorption experiments, Li et al. (2021a) confirmed a high affinity of K⁺ to exchangeable sites of two common clay minerals (kaolinite and smectite) at high pH (neutral to alkaline) due to hydroxyl deprotonation, causing higher δ^{41} K of adsorbed K⁺ than initial K⁺ and aqueous K⁺. This adsorption-driven isotopic fractionation may be important in the arid regolith, because exchangeable K (up to $\sim 35\%$) is important for regolith K budget, even in the intensely weathered samples. Collectively, clay formation processes (incorporation vs. sorption) may be responsible for distinct isotopic patterns in the regolith during chemical weathering. We propose that clay incorporation seems to dominate in the humid regolith in a circumneutral-acidic setting (pH = 5.4–6.4, unfavorable for K^+ sorption), producing lighter bulk isotopic composition ($\delta^{41}K_{ave}=-0.53\%$) than the basaltic substrate. Clay sorption likely dominates in the arid regolith in an alkaline setting (pH = 7.7–8.7), causing heavier K ($\delta^{41}K_{ave}=-0.28\%$) than the basaltic substrate (–0.48%, Fig. 5d). Hence, we infer that climate-dependent clay formation potentially controls terrestrial $\delta^{41}K$ records.

Exchangeable (NH₄Ac-extracted) K exhibits higher δ⁴¹K than that of the bulk in both regoliths (except for a humid, subsurface sample BE2). In comparison to the humid regolith, there is a high fraction of exchangeable K in the arid regolith (Fig. 2c). Hence, the preferential sorption of 41K on clays probably becomes important in the arid regolith, resulting in exchangeable K isotopically heavier than that of the bulk. The highest $\delta^{41}K$ of $-0.02 \pm 0.06\%$ occurs at the carbonate-enriched layer in the arid regolith. It is possible that downward infiltrating meteoric water and marine sprays passing through the regolith leave seawater δ^{41} K imprint at the carbonate zone during clay formation, and there are two plausible explanations. First, the marine imprint might be better preserved in the arid regolith (e.g., through sorption due to high pH, Li et al., 2021a) because soil solutions become concentrated and dissolved species remain within the regolith (Ziegler et al., 2003) rather than being removed by leaching (i.e., negative water balance, Goodfellow et al., 2014). In addition to the impact of sorption, isotopically heavy K derived from marine aerosols may be associated with carbonates (or other evaporitic deposits, as discussed in section 5.1), resulting in its bulk δ^{41} K close to the seawater δ^{41} K ($\sim 0.14\%$, Hille et al., 2019; Wang et al., 2020).

5.3. Plant cycling

Regolith K composition might be biologically influenced because K is a macronutrient and actively cycled by plants (uptake-return cycles of inorganic nutrients from depth to surface soils, Uhlig et al., 2020; Schlesinger, 2021). Because plant-used nutrients are continuously returned to the forest floor in litterfall, we may expect plant-cycled K to be gradually concentrated in surface horizons over time. This mechanism could be supported by the K enrichment (τ_K, Nb > 0) observed at the (sub)surface soil of humid regolith (Fig. 2). In Hawaiian soils, marine aerosol K is dilute and can be easily assimilated into roots. Therefore, plant cycling probably creates a feedback loop where seawater-derived K may be concentrated in soil organic matter and become influential in near surface horizons. As a consequence, the surface soil horizon in the humid site shows significant K enrichment ($\tau_{K,Nb} = 0.93$), which cannot be ascribed only to mineral aerosol addition (i.e., $\tau_{K,Nb} = 0.49$ of UCC, normalized to the Pololū basalt, Rudnick and Gao, 2013). Hence, surface K enrichment in the humid regolith probably reflects the contribution from both mineral aerosols

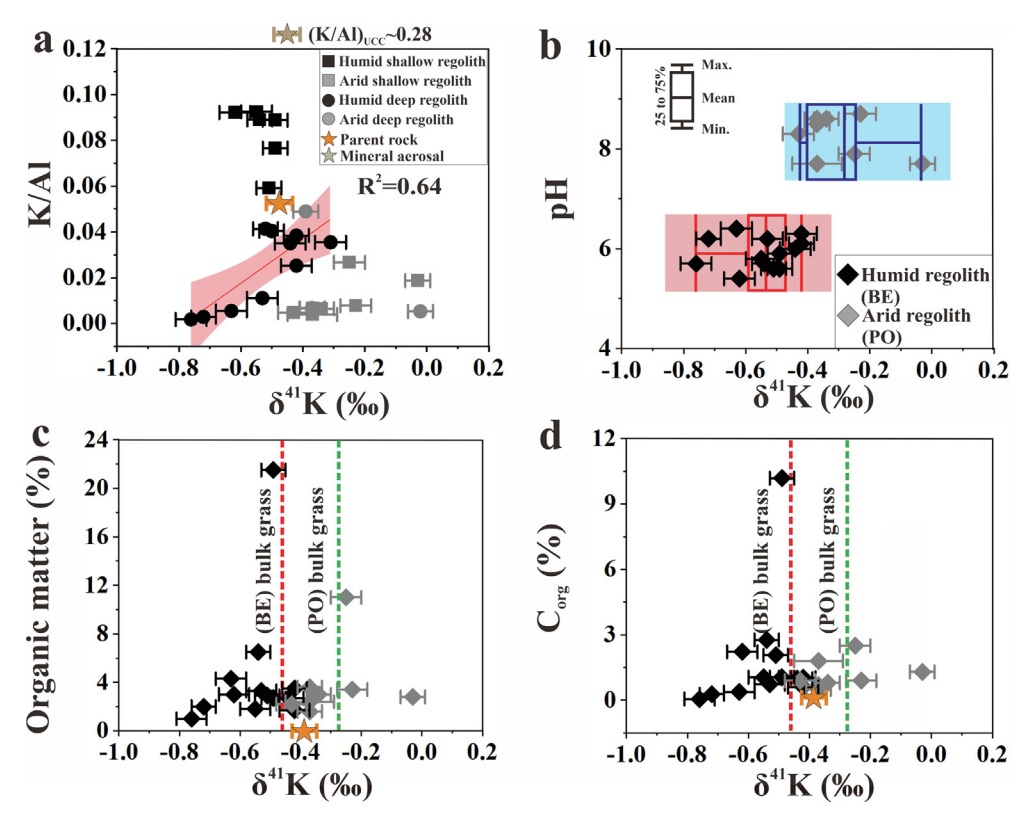


Fig. 5. Interrelationship of $\delta^{41}K$ with (a) K/Al, (b) pH, (c) organic matter content and (d) organic carbon (C) content. The composition of the pololū basalt is marked by an orange star. The data of humid and arid regoliths are symbolized using black and grey diamonds (95% c.i. uncertainty), respectively. In plot (a), the composition of mineral aerosols is provided in Rudnick and Gao (2013) ((K/Al)_{UCC} \sim 0.28) and Huang et al. (2020) ($\delta^{41}K_{UCC}$: 0.44 \pm 0.05‰). The linear correlation of humid deep regolith samples and corresponding 95% confidence interval is provided. Data in plot (b) are divided by boxplots (blue indicates acidic - humid, and orange indicates alkaline - arid). In plots (c-d), $\delta^{41}K$ values of bulk grass species (a sum of shoots and roots) growing in the humid (red, *P. setaceum*) and arid (green, *C. ciliaris*) sites are from Li et al. (2021c). We note that $\delta^{41}K$ values of bulk tree species are unknown. (Data tabulated in Tables 1–2 and supplementary data 2).

and plant cycling (K derived from marine aerosols, Chadwick et al., 1999; Bullen and Chadwick, 2016). Bouchez et al. (2013) also suggested that plant cycling of nutrients potentially influences soil isotope composition if (1) plant uptake flux is non-negligible relative to leaching loss, and (2) a fraction of the biomass can be preserved in soils. Thus, additional evidence of plant imprint comes from a linkage between the K isotope composition in the shallow regolith and plants.

If plant cycling matters for K isotope values, the bulk $\delta^{41}K$ value should be close to the $\delta^{41}K$ value of bulk plants due to the continuous accumulation of dead organic matter. This process may be illustrated by the link between soil organic matter (or organic carbon) and $\delta^{41}K$ (Fig. 5c and d). For example, in the humid regolith, the topmost soil with the highest content of organic matter (21.5%) and organic carbon (11.2%) has a δ^{41} K value of -0.49%, similar to that of the bulk grass (i.e., taken as an important part of litters added in soils, Li et al., 2021c). We note that bulk tree δ^{41} K is not available because tree roots were not sampled in Li et al. (2021c). This plant K imprint on organicenriched surface horizons can also be identified in the arid site (Fig. 5c and d). Through vegetative decay, plant-used K can be released into porewater, which is

quasi-equilibrium with exchangeable K (NH₄Ac extractable K). Indeed, we notice that NH₄Ac-K of humid surface soil is isotopically similar to bulk-plant K composition. The NH₄Ac-K of humid subsoil (BE 2, 17.5 cm) shows δ^{41} K close to bulk grass δ^{41} K (a sum of leaves, stems and roots based on weight average, -0.47%, Li et al., 2021c), but lower than that of NH₄Ac-K from lower horizons probably due to the overprint of seawater-derived K (discussed in Section 5.1).

5.4. Implications and perspectives

A consensus reported in previous studies is that the K isotope composition in solid weathering residuum would become lighter as weathering intensified (e.g., S. Li et al., 2019; Chen et al., 2019; Huang et al., 2020; Teng et al., 2020). As for long-term stable K reservoirs, clays in sediments and regoliths may serve as important ³⁹K pools for balancing oceanic sinks and hydrothermal inputs (Parendo et al., 2017; S. Li et al., 2019; Teng et al., 2020; Hu et al., 2020; Santiago Ramos et al., 2020). However, this study illustrates that K elemental and isotopic composition in the arid and humid regoliths in Hawai'i are determined by complex processes than previously studied humid.

(sub)tropical settings (Chen et al., 2019; Teng et al., 2020). Two distinct K isotope fractionation mechanisms under contrasting the climate conditions are involved: (1) the arid regolith, where positive K isotope fractionation from the basaltic substrate is ascribed to clay $^{41}\mathrm{K}$ adsorption and preservation of seawater K; and (2) the humid regolith, where dust-derived K dominate the shallow regolith and negative isotopic excursion in the lower unit may be caused by clay uptake of light K. Regolith K budget may be modulated by source mixing with basaltic components and atmospheric inputs linked to climate and may be affected by plant cycling. Thus, terrestrial $\delta^{41}\mathrm{K}$ records may be used as a proxy to better understand weathering processes and climate (humid vs. arid) based on the directionality of fractionation.

This study together with others (Santiago Ramos et al., 2018; S. Li et al., 2019, Chen et al., 2019; Teng et al., 2020; Li et al., 2021a; X. Li et al., 2022), show a wide δ^{41} K variation (>1‰) caused by Earth surface processes. Interpretation of the source and isotope fractionation of K during chemical weathering helps us to understand wide K isotope variations in river waters (S. Li et al., 2019; Wang et al., 2021; X. Li et al., 2022). In a more humid climate, stronger leaching may lead to more advanced weathering and higher output flux of ⁴¹K to river and groundwater systems. Isotopically light K may be preferentially incorporated into clays, generating river water (and groundwater) K fluxes with high δ^{41} K. The output of isotopically heavier K is consistent with a scenario outlined by S. Li et al. (2019) given a negative correlation between δ^{41} K in river water and the indices of weathering intensity based on river sediments. In comparison, occasional wetting events followed by rapid evapotranspiration in arid environments may prefer to retain heavy K in the regolith and limit K fluxes into groundwater and its contribution to stream flow (Hsieh et al. 1998). We hypothesize that seasonal (climatic) changes from dry to wet may introduce isotopically heavy K into waters due to (1) desorption of pre-sorbed heavy K from the regolith, and (2) clay incorporation of light K. It is still unclear to what extent our findings could be generalized to other terrestrial environments with different climate conditions. Because Hawai'i only represents a tropical island environment close to the oceans, future studies focusing on K isotopes in continental interior environments are needed.

6. CONCLUSIONS

This study provides detailed information of K chemistry in two regolith profiles developed on a homogeneous basaltic substrate sampled from a humid and an arid site in the big Island of Hawai'i. The results emphasize that the variation in measured $\delta^{41}K$ is mainly created by an interplay of atmospheric inputs, chemical weathering (particularly clay formation), and plant cycling, and climate has the potential to produce distinct terrestrial $\delta^{41}K$ records. The shallow regolith in the humid site shows upward K enrichment and $\delta^{41}K$ close to the upper crustal $\delta^{41}K$, revealing mineral aerosols imprint positively linked to local rainfall. In contrast, the arid shallow regolith loses most of its K. In addition, exchangeable (NH₄Ac extracts) K has $\delta^{41}K$ higher than the

bulk value in most regolith samples, likely due to the replenishment of marine aerosols. The enrichment of K in humid surface soils and upward decreasing $\delta^{41} K_{\rm NH4Ac}$ in the humid regolith and plant-like ⁴¹K in the topmost, organic-rich soils in both sites likely support the contribution of plant cycling. Light K isotope composition in humid, deep regolith relative to the basaltic substrate may be ascribed to preferential clay ³⁹K uptake in a circumneutral-acidic setting in Hawai'i. In comparison, heavy K isotope composition in the arid regolith relative to the substrate reflects an interplay between clay ⁴¹K sorption in an alkaline setting and the preservation of seawater K associated with clay adsorbed and carbonate phases in an evaporitic environment in Hawai'i. This study confirms that regolith K isotope composition is controlled by climate, thus making terrestrial K isotope records a promising tracer of weathering.

DECLARATION OF COMPETING INTEREST

The authors declare that they have no known competing financial interests or personal relationships that could have appeared to influence the work reported in this paper.

ACKNOWLEDGEMENTS

The authors acknowledge funding support from the NSF Career Award (EAR-1848153) to X.-M. Liu. We thank Brian W. Stewart for editorial handling and three anonymous reviewers, whose constructive comments significantly improve the paper.

APPENDIX A. SUPPLEMENTARY MATERIAL

Supplementary material to this article can be found online at https://doi.org/10.1016/j.gca.2022.07.001.

REFERENCES

An S., Luo X. and Li W. (2022) Precise measurement of 41 K/39 K ratios by HR-MC-ICP-MS under a dry and hot plasma setting. *Rapid Commun. Mass Spectrom.* 36, e9289.

Bataille C. P., Willis A., Yang X. and Liu X. M. (2017) Continental igneous rock composition: A major control of past global chemical weathering. *Sci. Adv.* 3, e1602183.

Berner E. K. and Berner R. A. (2012) *Global Environment: Water, Air, and Geochemical Cycles*. Princeton University Press.

Bouchez J., Von Blanckenburg F. and Schuessler J. A. (2013) Modeling novel stable isotope ratios in the weathering zone. *Am. J. Sci.* **313**, 267–308.

Bullen T. D. and Chadwick O. A. (2016) Ca, Sr and Ba stable isotopes reveal the fate of soil nutrients along a tropical climosequence. *Chem. Geol.* **422**, 25–45.

Brimhall G. H. and Dietrich W. E. (1987) Constitutive mass balance relations between chemical composition, volume, density, porosity, and strain in metasomatic hydrochemical systems: results on weathering and pedogenesis. *Geochim. Cosmochim. Acta* 51, 567–587.

Capo R. C., Whipkey C. E., Blachère J. R. and Chadwick O. A. (2000) Pedogenic origin of dolomite in a basaltic weathering profile, Kohala peninsula, Hawaii. *Geology* 28, 271–274.

Chadwick O. A., Derry L. A., Vitousek P. M., Huebert B. J. and Hedin L. O. (1999) Changing sources of nutrients during four million years of ecosystem development. *Nature* 397, 491–497.

- Chadwick O. A., Gavenda R. T., Kelly E. F., Ziegler K., Olson C. G., Elliott W. C. and Hendricks D. M. (2003) The impact of climate on the biogeochemical functioning of volcanic soils. *Chem. Geol.* 202, 195–223.
- Chadwick O. A., Derry L. A., Bern C. R. and Vitousek P. M. (2009) Changing sources of strontium to soils and ecosystems across the Hawaiian Islands. *Chem. Geol.* 267, 64–76.
- Chen H., Tian Z., Tuller-Ross B., Korotev R. L. and Wang K. (2019) High-precision potassium isotopic analysis by MC-ICP-MS: an inter-laboratory comparison and refined K atomic weight. *J. Anal. At. Spectrom.* 34, 160–171.
- Christensen J. N., Qin L., Brown S. T. and DePaolo D. J. (2018) Potassium and calcium isotopic fractionation by plants (soybean [Glycine max], rice [Oryza sativa], and wheat [Triticum aestivum]). ACS Earth Space Chem. 2, 745–752.
- DePaolo D. J. (1986) Detailed record of the Neogene Sr isotopic evolution of seawater from DSDP Site 590B. Geology 14, 103– 106
- Derry L. A. and Chadwick O. A. (2007) Contributions from Earth's atmosphere to soil. *Elements* 3, 333–338.
- Dohrmann R. (2006) Problems in CEC determination of calcareous clayey sediments using the ammonium acetate method. J. Plant Nutr. Soil Sci. 169, 330–334.
- Dupré B., Dessert C., Oliva P., Goddéris Y., Viers J., François L., Millot R. and Gaillardet J. (2003) Rivers, chemical weathering and Earth's climate. *Comptes Rendus Geosci.* 335, 1141–1160.
- Giambelluca T. W., Chen Q., Frazier A. G., Price J. P., Chen Y. L., Chu P. S., Eischied J. K. and Delparte D. M. (2013) Online rainfall atlas of Hawai'i. *Bull. Am. Meteor. Soc.* 94, 313–316.
- Goodfellow B. W., Chadwick O. A. and Hilley G. E. (2014) Depth and character of rock weathering across a basaltic-hosted climosequence on Hawai 'i. Earth Surf. Process. Landf. 39, 381– 398
- Hille M., Hu Y., Huang T. Y. and Teng F. Z. (2019) Homogeneous and heavy potassium isotope composition of global oceans. *Sci. Bull.* **64**, 1740–1742.
- Hindshaw R. S., Tosca R., Got T. L., Farnan I., Tosca N. J. and Tipper E. T. (2019) Experimental constraints on Li isotope fractionation during clay formation. *Geochim. Cosmochim.* Acta 250, 219–237.
- Hodell D. A., Mead G. A. and Mueller P. A. (1990) Variation in the strontium isotopic composition of seawater (8 Ma to present): Implications for chemical weathering rates and dissolved fluxes to the oceans. *Chem. Geol.* **80**, 291–307.
- Hsieh J. C. C., Chadwick O. A., Kelly E. F. and Savin S. M. (1998) Oxygen isotopic composition of soil water: Quantifying evaporation and transpiration. *Geoderma* 82, 269–293.
- Hu D., Clift P. D., Wan S., Bxning P., Hannigan R., Hillier S. and Blusztajn J. (2016) Testing chemical weathering proxies in Miocene-Recent fluvial-derived sediments in the South China Sea. *Geol. Soc. Spec. Publ.* **429**, 45–72.
- Hu Y., Chen X. Y., Xu Y. K. and Teng F. Z. (2018) High-precision analysis of potassium isotopes by HR-MC-ICPMS. *Chem. Geol.* 493, 100–108.
- Hu Y., Teng F. Z., Plank T. and Chauvel C. (2020) Potassium isotopic heterogeneity in subducting oceanic plates. Sci. Adv. 6), eabb2472.
- Hu Y., Teng F. Z., Helz R. T. and Chauvel C. (2021) Potassium isotope fractionation during magmatic differentiation and the composition of the mantle. J. Geophys. Res. Solid Earth 126, e2020IB021543
- Huang T. Y., Teng F. Z., Rudnick R. L., Chen X. Y., Hu Y., Liu Y. S. and Wu F. Y. (2020) Heterogeneous potassium isotope composition of the upper continental crust. *Geochim. Cosmochim. Acta* 278, 122–136.

- Kennedy M. J., Chadwick O. A., Vitousek P. M., Derry L. A. and Hendricks D. M. (1998) Changing sources of base cations during ecosystem development, Hawaiian Islands. *Geology* 26, 1015–1018.
- Kurtz A. C., Derry L. A., Chadwick O. A. and Alfano M. J. (2000) Refractory element mobility in volcanic soils. *Geology* 28, 683–686.
- Kurtz A. C., Derry L. A. and Chadwick O. A. (2001) Accretion of Asian dust to Hawaiian soils: isotopic, elemental, and mineral mass balances. *Geochim. Cosmochim. Acta* 65, 1971–1983.
- Kyte F. T., Leinen M., Heath G. R. and Zhou L. (1993) Cenozoic sedimentation history of the central North Pacific: Inferences from the elemental geochemistry of core LL44-GPC3. *Geochim. Cosmochim. Acta* 57, 1719–1740.
- Lasaga A. C., Soler J. M., Ganor J., Burch T. E. and Nagy K. L. (1994) Chemical weathering rate laws and global geochemical cycles. *Geochim. Cosmochim. Acta* 58, 2361–2386.
- Leinen M., Prospero J. M., Arnold E. and Blank M. (1994) Mineralogy of aeolian dust reaching the North Pacific Ocean: 1. Sampling and analysis. J. Geophys. Res. 99, 21017–21023.
- Li S., Li W., Beard B. L., Raymo M. E., Wang X., Chen Y. and Chen J. (2019a) K isotopes as a tracer for continental weathering and geological K cycling. *Proc. Natl. Acad. Sci.* U. S. A. 116, 8740–8745.
- Li W., Beard B. L. and Li S. (2016) Precise measurement of stable potassium isotope ratios using a single focusing collision cell multi-collector ICP-MS. J. Anal. At. Spectrom. 31, 1023–1029.
- Li W., Liu X. M. and Godfrey L. V. (2019b) Optimisation of lithium chromatography for isotopic analysis in geological reference materials by MC-ICP-MS. *Geostand. Geoanal. Res.* 43, 261–276.
- Li W., Liu X. M. and Chadwick O. A. (2020a) Lithium isotope behavior in Hawaiian regoliths: Soil-atmosphere-biosphere exchanges. *Geochim. Cosmochim. Acta* 285, 175–192.
- Li W., Liu X. M., Hu Y., Teng F. Z. and Hu Y. (2021a) Potassium isotopic fractionation during clay adsorption. *Geochim. Cos-mochim. Acta* 304, 160–177.
- Li W., Liu X. M., Wang K. and Koefoed P. (2021b) Lithium and potassium isotope fractionation during silicate rock dissolution: An experimental approach. *Chem. Geol.* 568, 120142.
- Li W., Liu X. M., Hu Y., Teng F. Z., Hu Y. F. and Chadwick O. A. (2021c) Potassium isotopic fractionation in a humid and an arid soil-plant system in Hawai 'i. *Geoderma* 400, 115219.
- Li W., Liu X. M., Wang K., Hu Y., Suzuki A. and Yoshimura T. (2022a) Potassium incorporation and isotope fractionation in cultured scleractinian corals. *Earth Planet. Sci. Lett.* 581, 117393.
- Li, W., Liu, X. M., Wang, K., Takahashi, Y., Hu, Y. and Chadwick, O. A. (2022b) Soil potassium isotope composition during four million years of ecosystem development in Hawai 'i. Geochim. Cosmochim. Acta (in press).
- Li X., Han G., Zhang Q. and Miao Z. (2020b) An optimal separation method for high-precision K isotope analysis by using MC-ICP-MS with a dummy bucket. *J. Anal. At. Spectrom.* **35**, 1330–1339.
- Li X., Han G., Liu M., Liu J., Zhang Q. and Qu R. (2022c) Potassium and its isotope behaviour during chemical weathering in a tropical catchment affected by evaporite dissolution. *Geochim. Cosmochim. Acta* 316, 105–121.
- Liu X. M. and Rudnick R. L. (2011) Constraints on continental crustal mass loss via chemical weathering using lithium and its isotopes. *Proc. Natl. Acad. Sci. U. S. A.* 108, 20873–20880.
- McDougall I. (1964) Potassium-argon ages from lavas of the Hawaiian Islands. *Geol. Soc. Am. Bull.* **75**, 107–128.
- Meybeck M. (1987) Global chemical weathering of surficial rocks estimated from river dissolved loads. *Am. J. Sci.* **287**, 401–428.

- Moore J. G. and Clague D. A. (1992) Volcano growth and evolution of the island of Hawaii. *Geol. Soc. Am. Bull.* **104**, 1471–1484.
- Morgan L. E., Ramos D. P. S., Davidheiser-Kroll B., Faithfull J., Lloyd N. S., Ellam R. M. and Higgins J. A. (2018) High-precision $^{41}\text{K}/^{39}\text{K}$ measurements by MC-ICP-MS indicate terrestrial variability of $\delta^{41}\text{K}$. J. Anal. At. Spectrom. 33, 175–186.
- Moynier F., Hu Y., Wang K., Zhao Y., Gérard Y., Deng Z., Moureau J., Li W., Simon J. I. and Teng F. Z. (2021) Potassium isotopic composition of various samples using a dual-path collision cell-capable multiple-collector inductively coupled plasma mass spectrometer, Nu instruments Sapphire. *Chem. Geol.* 571, 120144.
- Nakai S. I., Halliday A. N. and Rea D. K. (1993) Provenance of dust in the Pacific Ocean. Earth Planet. Sci. Lett. 119, 143–157.
- Nier A. O. (1938) The isotopic constitution of strontium, barium, bismuth, thallium and mercury. *Phys. Rev.* **54**, 275.
- Parendo C. A., Jacobsen S. B. and Wang K. (2017) K isotopes as a tracer of seafloor hydrothermal alteration. *Proc. Natl. Acad. Sci. U. S. A.* 114, 1827–1831.
- Parrington J. R., Zoller W. H. and Aras N. K. (1983) Asian dust: Seasonal transport to the Hawaiian Islands. Science 220, 195– 197
- Pettke T., Halliday A. N. and Rea D. K. (2002) Cenozoic evolution of Asian climate and sources of Pacific seawater Pb and Nd derived from eolian dust of sediment core LL44-GPC3. *Paleoceanography* 17, 3–11.
- Peucker-Ehrenbrink B., Ravizza G. and Hofmann A. W. (1995) The marine ¹⁸⁷Os/¹⁸⁶Os record of the past 80 million years. *Earth Planet. Sci. Lett.* **130**, 155–167.
- Porder S., Hilley G. E. and Chadwick O. A. (2007) Chemical weathering, mass loss, and dust inputs across a climate by time matrix in the Hawaiian Islands. *Earth Planet. Sci. Lett.* 258, 414–427.
- Pierson-Wickmann A. C., Reisberg L. and France-Lanord C. (2002) Behavior of Re and Os during low-temperature alteration: Results from Himalayan soils and altered black shales. *Geochim. Cosmochim. Acta* **66**, 1539–1548.
- Ravizza G. (1993) Variations of the ¹⁸⁷Os/¹⁸⁶Os ratio of seawater over the past 28 million years as inferred from metalliferous carbonates. *Earth Planet. Sci. Lett.* **118**, 335–348.
- Riebe C. S., Kirchner J. W., Granger D. E. and Finkel R. C. (2001) Strong tectonic and weak climatic control of long-term chemical weathering rates. *Geology* 29, 511–514.
- Royer D. L., Berner R. A. and Park J. (2007) Climate sensitivity constrained by CO₂ concentrations over the past 420 million years. *Nature* 446, 530.
- Rudnick R. L. and Gao S. (2013) Composition of the Continental Crust. In *Treatise on Geochemistry*, second ed. Elsevier Inc., pp. 1–51.
- Ryu J. S., Vigier N., Lee S. W., Lee K. S. and Chadwick O. A. (2014) Variation of lithium isotope geochemistry during basalt weathering and secondary mineral transformations in Hawaii. *Geochim. Cosmochim. Acta* 145, 103–115.
- Santiago Ramos D. P., Morgan L. E., Lloyd N. S. and Higgins J. A. (2018) Reverse weathering in marine sediments and the geochemical cycle of potassium in seawater: Insights from the K isotope composition of deep-sea pore-fluids. *Geochim. Cosmochim. Acta* 236, 99–120.
- Santiago Ramos D. P., Coogan L. A., Murphy J. G. and Higgins J. A. (2020) Low-temperature oceanic crust alteration and the isotopic budgets of potassium and magnesium in seawater. *Earth Planet. Sci. Lett.* **541**, 116290.
- Schlesinger W. H. (2021) Some thoughts on the biogeochemical cycling of potassium in terrestrial ecosystems. *Biogeochemistry* **154**, 427–432.

- Spengler S. R. and Garcia M. O. (1988) Geochemistry of the Hawi lavas, Kohala volcano, Hawaii. Contrib. Mineral. Petrol. 99, 90–104.
- Stewart B. W., Capo R. C. and Chadwick O. A. (2001) Effects of precipitation on weathering rate, base cation provenance and Sr isotope composition in a volcanic soil climosequence, Hawaii. *Geochim. Cosmochim. Acta* 65, 1087–1099.
- Teng F. Z., Hu Y., Ma J. L., Wei G. J. and Rudnick R. L. (2020) Potassium isotope fractionation during continental weathering and implications for global K isotopic balance. *Geochim. Cosmochim. Acta* 278, 261–271.
- Tuller-Ross B., Savage P. S., Chen H. and Wang K. (2019) Potassium isotope fractionation during magmatic differentiation of basalt to rhyolite. *Chem. Geol.* 525, 37–45.
- Uhlig D., Amelung W. and von Blanckenburg F. (2020) Mineral nutrients sourced in deep regolith sustain long-term nutrition of mountainous temperate forest ecosystems. *Global Biogeochem*. Cy. 34, e2019GB006513.
- Vance D., Teagle D. A. and Foster G. L. (2009) Variable Quaternary chemical weathering fluxes and imbalances in marine geochemical budgets. *Nature* 458, 493–496.
- Vigier N. and Goddéris Y. (2015) A new approach for modeling Cenozoic oceanic lithium isotope paleo-variations: the key role of climate. Clim. Past 11, 635–645.
- Vitousek P. M., Kennedy M. J., Derry L. A. and Chadwick O. A. (1999) Weathering versus atmospheric sources of strontium in ecosystems on young volcanic soils. *Oecologia* 121, 255–259.
- Vogel C., Helfenstein J., Massey M. S., Sekine R., Kretzschmar R., Beiping L., Peter T., Chadwick O. A., Tamburini F., Rivard C., Herzel H., Adam C., Pradas del Real A. E., Castillo-Michel H., Zuin L., Wang D., Félix R., Lassalle-Kaiser B. and Frossard E. (2021) Microspectroscopy reveals dust-derived apatite grains in acidic, highly-weathered Hawaiian soils. *Geoderma* 381, 114681.
- Wang K. and Jacobsen S. B. (2016) An estimate of the Bulk Silicate Earth potassium isotope composition based on MC-ICPMS measurements of basalts. *Geochim. Cosmochim. Acta* 178, 223– 232
- Wang K., Close H. G., Tuller-Ross B. and Chen H. (2020) Global average potassium isotope composition of modern seawater. ACS Earth Space Chem. 4, 1010–1017.
- Wang K., Peucker-Ehrenbrink B., Chen H., Lee H. and Hasenmueller E. A. (2021) Dissolved potassium isotopic composition of major world rivers. *Geochim. Cosmochim. Acta* 294, 145–159.
- Whipkey C. E., Capo R. C., Hsieh J. C. and Chadwick O. A. (2002) Development of magnesian carbonates in Quaternary soils on the Island of Hawaii. *J. Sediment. Res.* **72**, 158–165.
- Wiegand B. A., Chadwick O. A., Vitousek P. M. and Wooden J. L. (2005) Ca cycling and isotopic fluxes in forested ecosystems in Hawaii. *Geophy. Res. Lett.* 32, L11404.
- Xu Y. K., Hu Y., Chen X. Y., Huang T. Y., Sletten R. S., Zhu D. and Teng F. Z. (2019) Potassium isotopic compositions of international geological reference materials. *Chem. Geol.* 513, 101–107.
- Zhang W., Chen J., Ji J. and Li G. (2016) Evolving flux of Asian dust in the North Pacific Ocean since the late Oligocene. *Aeolian Res.* 23, 11–20.
- Zheng X. Y., Chen X. Y., Ding W., Zhang Y., Charin S. and Gérard Y. (2022a) High precision analysis of stable potassium (K) isotopes by the collision cell MC-ICP-MS "Sapphire" and a correction method for concentration mismatch. *J. Anal. At.* Spectrom. 37, 1273–1287.
- Zheng X. Y., Beard B. L., Neuman M., Fahnestock M. F., Bryce J. G. and Johnson C. M. (2022b) Stable potassium (K) isotope characteristics at mid-ocean ridge hydrothermal vents and its implications for the global K cycle. *Earth Planet. Sci. Lett.* 593, 117653.

Ziegler K., Hsieh J. C., Chadwick O. A., Kelly E. F., Hendricks D. M. and Savin S. M. (2003) Halloysite as a kinetically controlled end product of arid-zone basalt weathering. *Chem. Geol.* 202, 461–478.

Zieman J. J., Holmes J. L., Connor D., Jensen C. R. and Zoller W. H. (1995) Atmospheric aerosol trace element chemistry at Mauna Loa Observatory. J. Geophys. Res. 100, 25979–25994.

Associate editor: Brian W. Stewart